On the Performance of SSK Modulation over Correlated Nakagami-m Fading Channels

Marco Di Renzo, Harald Haas

On the Performance of SSK Modulation over Correlated Nakagami–*m* Fading Channels

Marco Di Renzo
French National Center for Scientific Research (CNRS)
Laboratory of Signals and Systems (LSS)
École Supérieure d'Électricité (SUPÉLEC)
3 rue Joliot–Curie, 91192 Gif–sur–Yvette (Paris), France
E–Mail: marco.direnzo@lss.supelec.fr

Harald Haas
The University of Edinburgh
Institute for Digital Communications (IDCOM)
College of Science and Engineering
Mayfield Road, Edinburgh, EH9 3JL, UK
E–Mail: h.haas@ed.ac.uk

Abstract— **In this paper, we develop an analytical framework for analyzing the performance of wireless systems adopting the recently proposed Space Shift Keying (SSK) modulation scheme. More specifically, we investigate the performance of a 2×1 MISO (Multiple–Input–Single–Output) system setup with Maximum–Likelihood (ML) detection at the receiver. The exact Average Bit Error Probability (ABEP) over correlated and non–identically distributed Nakagami–*m* fading channels is computed in closed–form. Numerical results will show that the performance of SSK modulation is significantly affected by the characteristics of fading channels, *e.g.*, channel correlation, fading severity, and power imbalance among the wireless links. Analytical frameworks and findings will also be substantiated via Monte Carlo simulations.**

I. Introduction

Space Shift Keying (SSK) and Spatial Modulation (SM) are two novel and recently proposed wireless transmission techniques for Multiple–Input–Multiple–Output (MIMO) wireless systems [1]–[4]. Recent research efforts have pointed out that they can be promising candidates to the design of low–complexity modulation schemes and transceiver architectures for MIMO systems over fading channels [5]–[7].

In particular, it has been shown that SSK and SM can offer better performance than other popular MIMO communication systems such as V–BLAST (Vertical Bell Laboratories Layered Space–Time) and Alamouti architectures, as well as Amplitude Phase Modulation (APM) schemes [5]–[7]. Furthermore, these performance gains are obtained with a significant reduction in receiver complexity and system design: SSK and SM can efficiently avoid Inter–Channel Interference (ICI) and Inter–Antenna Synchronization (IAS) issues of conventional MIMO systems, as well as reduce the number of computations required by the detection unit [5], [6]. Moreover, only one RF front–end chain is required, in theory, at the transmitter–side [7], which significantly reduces the overall complexity of the system. Furthermore, with respect to SM, SSK modulation can reduce further the receiver complexity owing to the absence of conventional modulation schemes for data transmission [7].

The fundamental and distinguishable feature that makes SSK and SM methods different from other MIMO techniques is the exploitation, as a source of information, of the spatial constellation pattern of the transmit–antennas[1]: the index of each transmit–antenna is encoded with a unique sequence of bits emitted by the transmit encoder, and data transmission is based upon the following fundamental principles: i) activate the transmit–antenna which is linked to the sequence of bits to be transmitted, and ii) switch off the rest of the transmit–antennas. This way, the estimation, at the receiver–side, of which antenna is not idle results, implicity, in the estimation of the unique sequence of bits emitted by the encoder at the transmitter–side. At the receiver–side, the detection mechanism of the antenna index is based upon the distinct multipath fading characteristics associated to each transmit–receive wireless link [1].

Numerical studies in, *e.g.*, [5], [7], have pointed out that the fundamental issue to be taken into account for the accurate analysis, design, and optimization of SSK and SM is channel correlation among the transmit–receive wireless paths. As a matter of fact, at the receiver–side, the optimal detector [6] is designed to exploit the distinct multipath profiles of different wireless links: if correlation exist among them, it may be unable to distinguish the different antennas, which will appear similar at the receiver. In order to cope with channel correlation, in [8] a novel scheme named Trellis Coded Spatial Modulation (TCSM) is introduced, which exploits trellis coding to reduce the effect of spatial correlation of the fading channel. However, all performance evaluations conducted in correlated fading scenarios for either SSK or SM schemes to date are based on Monte Carlo simulations, which only yield limited insights about the system performance. To the best of the authors knowledge, only in [9] the authors have attempted to develop an analytical framework to analyze the performance of SM over correlated Nakagami–*m* fading channels. However, this latter framework shows three main limitations: i) the detector is suboptimal, ii) the proposed method is semi–analytical, and, more important, iii) fading correlation is taken into account only for data detection, while the probability of transmit–antenna detection is computed by using the framework in [5], which neglects fading correlation.

Motivated by these considerations, in this paper we propose an exact analytical framework for the analysis of the performance of SSK modulation over Nakagami–*m* fading channels by explicitly taking into account the spatial correlation among the transmit–antennas. More specifically, we will focus our attention on the basic 2×1 MISO (Multiple–Input–Single–Output) system setup with Maximum–Likelihood (ML) detection at the receiver, and closed–form expressions for the Average Bit Error Probability (ABEP) will be provided. Although the system setup is the simplest one for SSK, it

[1]This is the only means to convey information for SSK modulation [7].

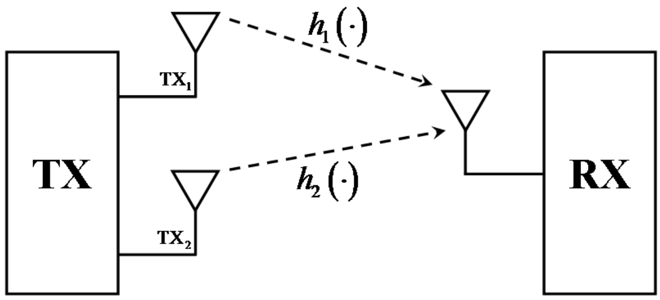

Fig. 1. System model: the 2×1 MISO setting.

represents the building block for performance analysis of more general MIMO systems[2]. For example, the performance of $M \times 1$ MISO systems, where M is the number of transmit–antennas, could be readily obtained via the very tight union–bound framework recently introduced in [12]. Our framework will point out that the system performance can be significantly affected by different channel fading conditions, and, in particular, by spatial correlation and power imbalance between the wireless links.

The remainder of the paper is organized as follows. In Section II, system and channel models are introduced. In Section III, the analytical framework for performance analysis over independent and correlated Nakagami–*m* fading is developed. In Section IV, numerical and simulation results are shown to substantiate the accuracy of the analytical framework. Finally, Section V concludes the paper.

II. System Model and Background

Let us consider the 2×1 MISO system depicted in Fig. 1. As mentioned in Section I, SSK–based transmission techniques foresee i) at the transmitted–side, to map information data bits to transmit–antenna indexes, and ii) at the receiver–side, to de–map these bits via suitable detection mechanisms for estimating, for each signaling time–interval, the active transmit–antenna. In particular, the detection process at the receiver–side can be cast in terms of a general binary detection problem in Additive White Gaussian Noise (AWGN) [13, Sec. 4.2, pp. 254], when conditioning upon fading channel statistics. In this section, we will briefly summarize the SSK detection problem and the ML optimum detector when the receiver has full Channel State Information (CSI) [6].

A. Notation

Let us briefly summarize the main notation used in what follows. i) We adopt a complex–envelope signal representation. ii) $j = \sqrt{-1}$ is the imaginary unit. iii) $(x \otimes y)(t) = \int_{-\infty}^{+\infty} x(\xi) y(t-\xi) d\xi$ is the convolution of signals $x(\cdot)$ and $y(\cdot)$. iv) $(\cdot)^*$ denotes complex–conjugate. v) $|\cdot|^2$ denotes square absolute value. vi) $\mathrm{E}\{\cdot\}$ is the expectation operator. vii) $\mathrm{Re}\{\cdot\}$ denotes the real part operator. viii) $\Pr\{\cdot\}$ means probability. ix) ρ_{AB} denotes the correlation coefficient of Random Variables (RVs) A and B. x) $Q(x) = \left(1/\sqrt{2\pi}\right)\int_x^{+\infty} \exp\left(-t^2/2\right) dt$ is the Q–function. xi) $\bar{m}_1$ and $\bar{m}_2$ denote the two information messages that the transmitter in Fig. 1 can emit with equal probability. xii) $\hat{m}$ denotes the message estimated at the receiver–side. xiii) $E_m = E_{\bar{m}_1} = E_{\bar{m}_2}$ is the energy transmitted by each antenna that emits a non–zero signal. xiv) $T_m = T_{\bar{m}_1} = T_{\bar{m}_2}$ denotes the signaling interval for both information messages $\bar{m}_1$ and $\bar{m}_2$. xv) The noise at the receiver input is denoted by $n(\cdot)$, and is assumed to be AWG–distributed, with both real and imaginary parts having a double–sided power spectral density equal to N_0. xvi) For ease of notation, we set $\bar{\gamma} = E_m/(4N_0)$. xvii) $\left\{ s_i \left(\cdot \middle| \{\bar{m}_n\}_{n=1}^2 \right) \right\}_{i=1}^2$ denote the signals emitted by the transmit–antennas $\{\mathrm{TX}_i\}_{i=1}^2$ conditioned upon the transmitted messages $\{\bar{m}_i\}_{i=1}^2$. xviii) $\Gamma(\cdot)$ is the Gamma function [14, Eq. (6.1.1)]. xix) $I_\nu(\cdot)$ is the modified Bessel function of first kind and order ν [14, Ch. 9)]. xx) $G_{p,q}^{m,n}\left(.\middle| \begin{array}{c} (a_p) \\ (b_q) \end{array} \right)$ is the Meijer–G function defined in [15, Ch. 8, pp. 519]. xxi) $\delta(\cdot)$ is the Dirac delta function.

B. Channel Model

We consider a frequency–flat slowly–varying fading channel model, with fading envelopes distributed according to a Nakagami–*m* distribution [16]. Moreover, we assume the fading gains not to be necessarily identically distributed, and spatial correlation among them will be accounted for in this manuscript. In particular:

- $\{h_i(t)\}_{i=1}^2 = \beta_i \exp(j\varphi_i)\,\delta(t-\tau_i)$ is the channel impulse response from antenna $\{\mathrm{TX}_i\}_{i=1}^2$ in Fig. 1 to the receive antenna, and $\{\beta_i\}_{i=1}^2$, $\{\varphi_i\}_{i=1}^2$, and $\{\tau_i\}_{i=1}^2$ denote gain, phase, and delay of the related wireless link. Moreover, $\{\alpha_i\}_{i=1}^2 = \beta_i \exp(j\varphi_i)$ denotes the channel complex–gain of the related wireless link.
- $\{\tau_i\}_{i=1}^2$ are assumed to be independent and uniformly distributed in $[0, T_m)$, but known at the receiver, *i.e.*, perfect time–synchronization is considered.
- $\{\varphi_i\}_{i=1}^2$ are assumed to be independent and uniformly distributed in $[0, 2\pi)$.
- The channel envelopes, $\{\beta_i\}_{i=1}^2$, are assumed to be distributed according to a bivariate Nakagami–*m* distribution with joint Probability Density Function (PDF), $f_{\beta_1,\beta_2}(\cdot,\cdot)$, as follows [16, Eq. (6.1)]:

$$\begin{aligned} f_{\beta_1,\beta_2}(\xi_1,\xi_2) = A \exp\left(-B_1\xi_1^2\right)\exp\left(-B_2\xi_2^2\right) \\ \times \xi_1^m \xi_2^m I_{m-1}(C\xi_1\xi_2) \end{aligned} \tag{1}$$

where we have defined:

$$\begin{cases} A = \dfrac{4m^{m+1}}{\Gamma(m)\,\Omega_1\Omega_2\left(1-\rho_{\beta_1^2\beta_2^2}\right)\left(\sqrt{\Omega_1\Omega_2\rho_{\beta_1^2\beta_2^2}}\right)^{m-1}} \\ \{B_i\}_{i=1}^2 = \dfrac{m}{\Omega_i\left(1-\rho_{\beta_1^2\beta_2^2}\right)} \\ C = \dfrac{2m\sqrt{\rho_{\beta_1^2\beta_2^2}}}{\sqrt{\Omega_1\Omega_2}\left(1-\rho_{\beta_1^2\beta_2^2}\right)} \end{cases} \tag{2}$$

with m denoting the Nakagami–*m* fading parameter and $\{\Omega_i\}_{i=1}^2 = \mathrm{E}\{\beta_i^2\}$.
In particular, for uncorrelated fading, *i.e.*, $\rho_{\beta_1^2\beta_2^2} = 0$, we have $f_{\beta_1,\beta_2}(\xi_1,\xi_2) = f_{\beta_1}(\xi_1) f_{\beta_2}(\xi_2)$, where $\{f_{\beta_i}(\cdot)\}_{i=1}^2$ are the PDFs of univariate Nakagami–*m* RVs

[2]Note that, when novel transmission technologies are proposed, is typical to analyze first the simplest system setup to develop the basic analytical tools. A recent example is the performance analysis of cooperative systems over fading channels, where the frameworks have evolved from [10] to [11].

[16, Eq. (2.20)]:

$$\{f_{\beta_i}(\xi_i)\}_{i=1}^2 = \tilde{A}_i \xi_i^{\tilde{C}_i} \exp\left(-\tilde{B}_i \xi_i^2\right) \quad (3)$$

where:

$$\begin{cases} \tilde{A}_i = \dfrac{2}{\Gamma(m_i)} \left(\dfrac{m_i}{\Omega_i}\right)^{m_i} \\ \tilde{B}_i = 2m_i - 1 \\ \tilde{C}_i = \dfrac{m_i}{\Omega_i} \end{cases} \quad (4)$$

Note that, for the uncorrelated case in (3), we have considered the general scenario where the Nakagami–*m* fading parameters m_1 and m_2 of the wireless links are not necessarily the same.

C. Binary Detection

Moving from the above system and channel model, the signals after propagation through the wireless fading channel for both wireless links are $\left\{\tilde{s}_i\left(t|\{\bar{m}_n\}_{n=1}^2\right)\right\}_{i=1}^2 = (s_i \otimes h_i)(t) = \beta_i \exp(j\varphi_i) s_i(t - \tau_i|\bar{m}_n)$, and the received signal can be written as follows:

$$\begin{cases} r(t|\bar{m}_1) = \tilde{s}_1(t|\bar{m}_1) + \tilde{s}_2(t|\bar{m}_1) + n(t) \\ r(t|\bar{m}_2) = \tilde{s}_1(t|\bar{m}_2) + \tilde{s}_2(t|\bar{m}_2) + n(t) \end{cases} \quad (5)$$

when messages $\bar{m}_1$ and $\bar{m}_2$ are transmitted, respectively. Note that (5) is a general hypothesis binary testing problem where both transmit–antennas could be activated when a message is transmitted [1], [17].

Accordingly, for SSK modulation the general binary detection problem in (6) can be formulated:

$$\begin{cases} r(t) = \bar{s}_1(t) + n(t) & \text{if } \bar{m}_1 \text{ is sent} \\ r(t) = \bar{s}_2(t) + n(t) & \text{if } \bar{m}_2 \text{ is sent} \end{cases} \quad (6)$$

where $\bar{s}_1(t) = \tilde{s}_1(t|\bar{m}_1) + \tilde{s}_2(t|\bar{m}_1)$ and $\bar{s}_2(t) = \tilde{s}_1(t|\bar{m}_2) + \tilde{s}_2(t|\bar{m}_2)$.

Moving from (6), the ML optimum detector with full–CSI and perfect synchronization at the receiver is as follows [13, Sec. 4.2, pp. 254, eq. (31)]:

$$\hat{m} = \begin{cases} \bar{m}_1 & \text{if } D_1 \geq D_2 \\ \bar{m}_2 & \text{if } D_2 < D_1 \end{cases} \quad (7)$$

where $\{D_i\}_{i=1}^2$ are the decision metrics defined in what follows:

$$\begin{cases} D_1 = \mathrm{Re}\left\{\displaystyle\int_{T_m} r(t)\, \bar{s}_1^*(t)\, dt\right\} - \dfrac{1}{2}\displaystyle\int_{T_m} \bar{s}_1(t)\, \bar{s}_1^*(t)\, dt \\ D_2 = \mathrm{Re}\left\{\displaystyle\int_{T_m} r(t)\, \bar{s}_2^*(t)\, dt\right\} - \dfrac{1}{2}\displaystyle\int_{T_m} \bar{s}_2(t)\, \bar{s}_2^*(t)\, dt \end{cases} \quad (8)$$

From the decision rule in (7), the probability of error, $\mathrm{P_E}$, of the detection process (*i.e.*, the detection of the index of the transmit–antenna), when conditioning upon the channel impulses responses $\{h_i(\cdot)\}_{i=1}^2$, is as follows:

$$\begin{aligned} \mathrm{P_E}(h_1, h_2) &= \frac{1}{2}\, \mathrm{P_E}(h_1, h_2)|_{\bar{m}_1} + \frac{1}{2}\, \mathrm{P_E}(h_1, h_2)|_{\bar{m}_2} \\ &= \frac{1}{2}\Pr\left\{ D_1|_{\bar{m}_1} < D_2|_{\bar{m}_1}\right\} + \frac{1}{2}\Pr\left\{ D_2|_{\bar{m}_2} < D_1|_{\bar{m}_2}\right\} \end{aligned} \quad (9)$$

where $\left\{\mathrm{P_E}(\cdot,\cdot)|_{\bar{m}_i}\right\}_{i=1}^2$ and $\left\{D_j|_{\bar{m}_i}\right\}_{i,j=1}^2$ denote the probabilities of error and the decision metrics conditioned upon the transmission of messages $\{\bar{m}_i\}_{i=1}^2$, respectively.

III. ABEP over Correlated Nakagami–*m* Fading Channels

According to [6], [7], for SSK modulation we have:

$$\begin{cases} \bar{s}_1(t) = \tilde{s}_1(t|\bar{m}_1) \\ \bar{s}_2(t) = \tilde{s}_2(t|\bar{m}_2) \end{cases} \quad (10)$$

which means that only one transmit–antenna is activated when either $\bar{m}_1$ or $\bar{m}_2$ have to be sent, *i.e.*, TX_1 or TX_2, respectively.

By either assuming that the transmitted signals are pure sinusoidal tones, *i.e.*, $s_1(t|\bar{m}_1) = s_2(t|\bar{m}_2) = \sqrt{E_m}$ and $s_1(t|\bar{m}_2) = s_2(t|\bar{m}_1) = 0$, or $\tau_1 \cong \tau_2$, which is a realistic assumption when the distance between transmitter and receiver is much larger than the spacing between the transmit–antennas, (6) simplifies as follows ($t \in [0, T_m)$):

$$\begin{cases} r(t|\bar{m}_1) = \beta_1\sqrt{E_m}\exp(j\varphi_1) + n(t) \\ r(t|\bar{m}_2) = \beta_2\sqrt{E_m}\exp(j\varphi_2) + n(t) \end{cases} \quad (11)$$

After some analytical computations, which are omitted in the present manuscript due to space constraints, $\mathrm{P_E}$ in (5) can be written as follows:

$$\mathrm{P_E}(h_1, h_2) = Q\left(\sqrt{\bar{\gamma}\,|\alpha_2 - \alpha_1|^2}\right) \quad (12)$$

which agrees with the result in [6].

The formula in (12) yields the BEP when conditioning upon fading channel statistics, *i.e.*, $\{\alpha_i\}_{i=1}^2$. In [6], [7] only uncorrelated Rayleigh fading is considered from the point of view of analytical modeling. In this section, we provide exact and closed–form expressions for performance analysis over correlated Nakagami–*m* fading.

In particular, the ABEP is computed by resorting to the well–known Moment Generating Function (MGF–) based approach for performance analysis of digital communication systems over fading channels [16]. Accordingly, by using [16, Eq. (5.1), Eq. (5.3)] and (12), the ABEP can be written as follows:

$$\mathrm{ABEP} = \mathrm{E}\{\mathrm{P_E}(h_1, h_2)\} = \frac{1}{\pi}\int_0^{\pi/2} M_\gamma\left(\frac{\bar{\gamma}}{2\sin^2(\theta)}\right) d\theta \quad (13)$$

where $M_\gamma(s) = \mathrm{E}\{\exp(-s\gamma)\}$ is the MGF of RV γ, and $\gamma = |\alpha_2 - \alpha_1|^2 = |\beta_2\exp(j\varphi_2) - \beta_1\exp(j\varphi_1)|^2$.

A. Computation of the MGF, $M_\gamma(\cdot)$, of γ

The MGF, $M_\gamma(\cdot)$, of γ, can be written as follows:

$$M_\gamma(s) = \int_0^{+\infty}\int_0^{+\infty} M_\gamma(s; \xi_1, \xi_2)\, f_{\beta_1,\beta_2}(\xi_1, \xi_2)\, d\xi_1 d\xi_2 \quad (14)$$

with $M_\gamma(\cdot; \cdot, \cdot)$ being defined as:

$$\begin{aligned} M_\gamma(s; \beta_1, \beta_2) = &\left(\frac{1}{2\pi}\right)^2 \exp\left(-s\beta_1^2\right)\exp\left(-s\beta_2^2\right) \\ &\times \int_0^{2\pi}\int_0^{2\pi} \exp\left[2s\beta_1\beta_2\cos(\phi_2 - \phi_1)\right] d\phi_1 d\phi_2 \end{aligned} \quad (15)$$

$$M_\gamma(s) = \tilde{A}_1\tilde{A}_2 \int_0^{+\infty} \xi_1^{\tilde{C}_1} \exp\left[-\left(s+\tilde{B}_1\right)\xi_1^2\right] \underbrace{\left[\int_0^{+\infty} \xi_2^{\tilde{C}_2} \exp\left[-\left(s+\tilde{B}_2\right)\xi_2^2\right] I_0\left(2s\xi_1\xi_2\right) d\xi_2\right]}_{J(s;\xi_1)} d\xi_1 \tag{18}$$

$$J(s;\xi_1) = \frac{1}{2}\int_0^{+\infty} \xi_2^{\left(\frac{1}{2}\tilde{C}_2-\frac{1}{2}\right)} G_{0,1}^{1,0}\left(\left(s+\tilde{B}_2\right)\xi_2 \middle| \begin{matrix} - \\ 0 \end{matrix}\right) G_{0,2}^{1,0}\left(-s^2\xi_1^2\xi_2 \middle| \begin{matrix} - \\ 0 \quad 0 \end{matrix}\right) d\xi_2 \tag{19}$$

$$M_\gamma(s) = A \int_0^{+\infty}\int_0^{+\infty} \xi_1^m \xi_2^m \exp\left[-\left(s+B_1\right)\xi_1^2\right] \exp\left[-\left(s+B_2\right)\xi_2^2\right] I_0\left(2s\xi_1\xi_2\right) I_{m-1}\left(C\xi_1\xi_2\right) d\xi_1 d\xi_2 \tag{22}$$

$$\Psi_h(s) = \int_0^{+\infty} \xi_1^{2m+2h-1} \exp\left[-\left(s+B_1\right)\xi_1^2\right] \underbrace{\left[\int_0^{+\infty} \xi_2^{2m+2h-1} \exp\left[-\left(s+B_2\right)\xi_2^2\right] I_0\left(2s\xi_1\xi_2\right) d\xi_2\right]}_{\Psi_h(s;\xi_1)} d\xi_1 \tag{24}$$

where we have taken into account that $\{\varphi_i\}_{i=1}^2$ are independent and uniformly distributed RVs in $[0, 2\pi)$, as described in Section II-B.

By using similar analytical steps as in [13, pp. 339, Eq. (366), Eq. (367)], the two–fold integral in (15) can be computed in closed–form as follows:

$$\int_0^{2\pi}\int_0^{2\pi} \exp\left[2s\beta_1\beta_2\cos\left(\phi_2-\phi_1\right)\right] d\phi_1 d\phi_2 = \left(2\pi\right)^2 I_0\left(2s\beta_1\beta_2\right) \tag{16}$$

thus yielding the simple expression in what follows for $M_\gamma(\cdot;\cdot,\cdot)$:

$$M_\gamma(s;\beta_1,\beta_2) = \exp\left(-s\beta_1^2\right)\exp\left(-s\beta_2^2\right) I_0\left(2s\beta_1\beta_2\right) \tag{17}$$

B. Uncorrelated Nakagami–m Fading

For uncorrelated fading, by using (3) and (17), the MGF, $M_\gamma(\cdot)$, of γ in (14) simplifies as shown in (18) on top of this page. In particular, the integral $J(\cdot;\cdot)$ within the square brackets in (18) can be re–written, by using [15, Eq. (8.4.3.1)], [15, Eq. (8.4.22)] and some algebraic manipulations, as shown in (19) on top of this page. Furthermore, the integral in (19) can be solved in closed–form by using the Mellin–Barnes theorem in [15, Eq. (2.24.1.1)], as shown in what follows:

$$J(s;\xi_1) = \frac{1}{2}\left(s+\tilde{B}_2\right)^{-\left(\frac{1}{2}+\frac{\tilde{C}_2}{2}\right)} G_{1,2}^{1,1}\left(-\frac{s^2\xi_1^2}{s+\tilde{B}_2} \middle| \begin{matrix} \frac{1}{2}-\frac{\tilde{C}_2}{2} \\ 0 \quad 0 \end{matrix}\right) \tag{20}$$

Finally, by substituting (20) into (18), and using again [15, Eq. (8.4.3.1)] along with the Mellin–Barnes theorem in [15, Eq. (2.24.1.1)], a closed–form expression for the MGF, $M_\gamma(\cdot)$, of γ, can be obtained as follows:

$$\begin{aligned} M_\gamma(s) = {} & \frac{\tilde{A}_1\tilde{A}_2}{4}\left(s+\tilde{B}_1\right)^{-\left(\frac{1}{2}+\frac{\tilde{C}_1}{2}\right)}\left(s+\tilde{B}_2\right)^{-\left(\frac{1}{2}+\frac{\tilde{C}_2}{2}\right)} \\ & \times G_{2,2}^{1,2}\left(-\frac{s^2}{\left(s+\tilde{B}_1\right)\left(s+\tilde{B}_2\right)} \middle| \begin{matrix} \frac{1}{2}-\frac{\tilde{C}_2}{2} & \frac{1}{2}-\frac{\tilde{C}_1}{2} \\ 0 & 0 \end{matrix}\right) \end{aligned} \tag{21}$$

C. Correlated Nakagami–m Fading

For correlated fading, by using (1) and (17), the MGF, $M_\gamma(\cdot)$, of γ, in (14) simplifies as shown in (22) on top of this page. By using the infinite series representation [14, Eq. (9.6.10)] of the $I_{m-1}(\cdot)$ Bessel function in (22), this latter integral can be re–written as shown in (23) in what follows:

$$M_\gamma(s) = \sum_{h=0}^{+\infty}\left[\frac{AC^{m+2h-1}}{2^{m-1}4^h\left(h!\right)\Gamma\left(h+m\right)}\Psi_h(s)\right] \tag{23}$$

where $\Psi_h(\cdot)$ is defined in (24) on top of this page.

By using the same analytical steps as for computing $J(\cdot;\cdot)$ in (19), the integral $\Psi_h(\cdot;\cdot)$ within the square brackets in (24) can be computed in closed–form as follows:

$$\Psi_h(s;\xi_1) = \frac{1}{2}\left(s+B_2\right)^{-(m+h)} G_{1,2}^{1,1}\left(-\frac{s^2\xi_1^2}{s+B_2} \middle| \begin{matrix} 1-m-h \\ 0 \quad 0 \end{matrix}\right) \tag{25}$$

Finally, by substituting (25) into (24), and using [15, Eq. (8.4.3.1)] along with the Mellin–Barnes theorem in [15, Eq. (2.24.1.1)], the integral $\Psi_h(\cdot)$ can be computed in closed–form as follows:

$$\begin{aligned} \Psi_h(s) = {} & \frac{A}{4}\left(s+B_1\right)^{-(m+h)}\left(s+B_2\right)^{-(m+h)} \\ & \times G_{2,2}^{1,2}\left(-\frac{s^2}{\left(s+B_1\right)\left(s+B_2\right)} \middle| \begin{matrix} 1-m-h & 1-m-h \\ 0 & 0 \end{matrix}\right) \end{aligned} \tag{26}$$

which, along with (23), yields the desired closed–form expression for computing the MGF, $M_\gamma(\cdot)$, of γ.

As a final remark, we observe that, although the final result in (23) requires an infinite series to compute the MGF, this series is absolutely convergent, and converges rapidly thanks to the factorial term and the Gamma function in its denominator, *i.e.*, only a few terms are required to obtain a good accuracy.

IV. Numerical and Simulation Results

In this section, we provide some numerical results with a twofold objective: i) to validate the accuracy of the analytical frameworks developed in Section III, and ii) to analyze the

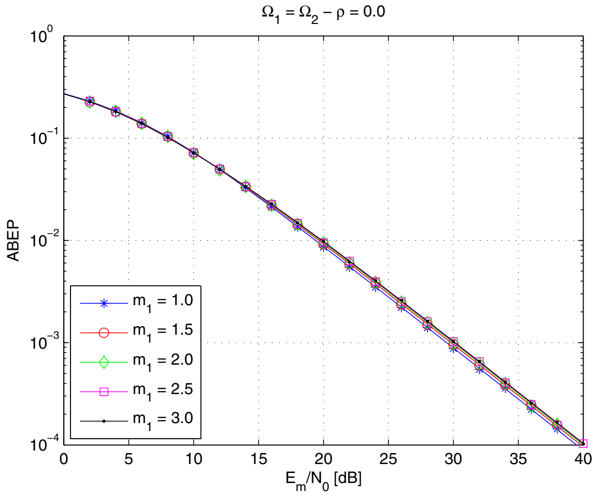

Fig. 2. Comparison between Monte Carlo simulation (markers) and analytical model (solid lines). Uncorrelated fading with balanced power ($m_2 = 2.0$).

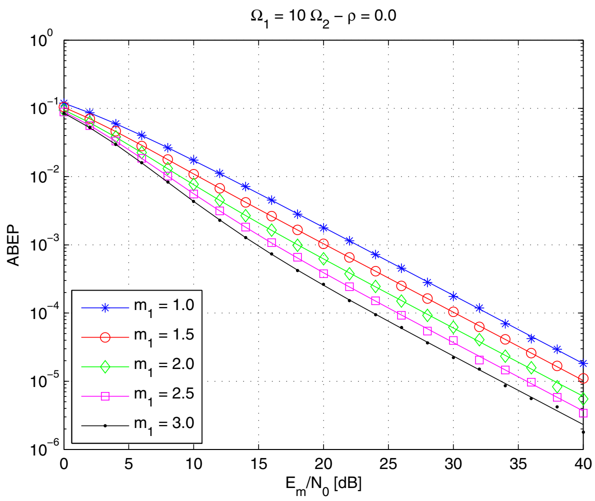

Fig. 3. Comparison between Monte Carlo simulation (markers) and analytical model (solid lines). Uncorrelated fading with unbalanced power ($m_2 = 2.0$).

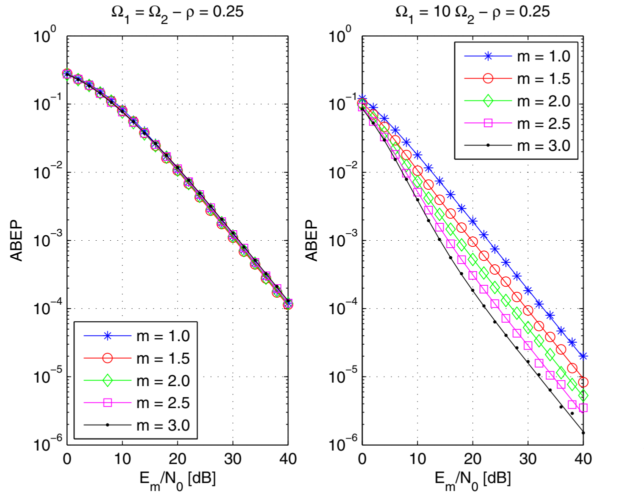

Fig. 4. Comparison between Monte Carlo simulation (markers) and analytical model (solid lines). Correlated fading with balanced power ($\rho = \rho_{\beta_1^2 \beta_2^2}$).

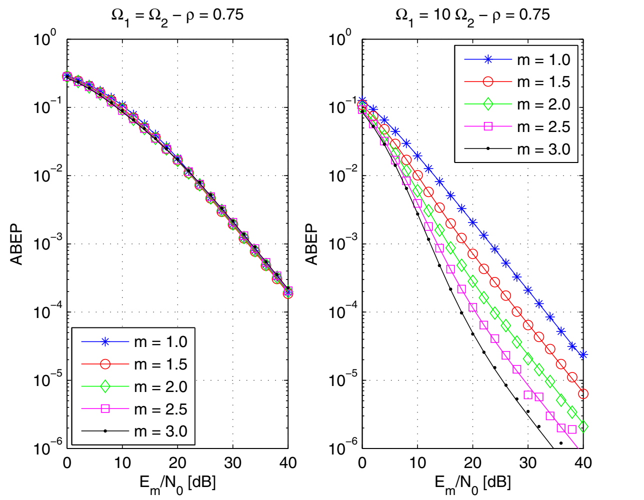

Fig. 5. Comparison between Monte Carlo simulation (markers) and analytical model (solid lines). Correlated fading with unbalanced power ($\rho = \rho_{\beta_1^2 \beta_2^2}$).

performance of SSK modulation for different fading scenarios (*e.g.*, the spatial correlation between the transmit–antennas). The system setup used to obtain the numerical examples is shown for each figure in its caption and title (with $\Omega_2 = 1$). In particular, we have analyzed the system performance for various fading parameters (m), for balanced and unbalanced (*i.e.*, $\Omega_1 \neq \Omega_2$) fading scenarios, as well as for various correlation coefficients. Monte Carlo simulations are obtained by using the simulation framework proposed in [18] to generate bivariate Nakagami–*m* fading envelopes[3]. Moreover, the series in (23) is truncated to the first 20 terms to get very accurate numerical estimates. Finally, from the MGFs in (21) and (23), the ABEP is obtained from (13) by using straightforward numerical integration techniques.

In Fig. 2 and Fig. 3, the scenario with uncorrelated fading for a balanced and an unbalanced setup is shown, respectively. By comparing the two figures, the following observations can be made: i) the proposed analytical model is very accurate and well overlaps with Monte Carlo simulations for various system settings, ii) the system performance improves for unbalanced fading as a result of (12), which shows that the system performance depends on the difference between the complex fading gains of the two wireless links, iii) when a balanced fading scenario is considered, the system performance is almost the same for various Nakagami–*m* fading parameters, *i.e.*, the system performance changes very little with the fading severity, and iv) on the other hand, for unbalanced fading the system performance improves significantly for less severe fading conditions (*i.e.*, m_1 increases). We also remark that similar conclusions can be drawn for different values of m_2, even though the results are not shown due to space constraints.

[3]Note that some typos in [18] have been adequately fixed and carefully taken into account to produce Monte Carlo simulation results.

In Fig. 4 and Fig. 5, the scenario with correlated fading for a low and high correlation coefficient is shown, respectively. By carefully analyzing the figures, the following observations can be made: i) also in this case, the proposed analytical model is very accurate and well overlaps with Monte Carlo simulations for various system settings, ii) similar to the uncorrelated scenario, SSK modulation offers better performance for unbalanced fading conditions, since, in this case, the multipath channels are more distinguishable from each other, iii) for a balanced fading setup, *i.e.*, $\Omega_1 = \Omega_2$, we note that the performance gets worse as the correlation coefficient increases, as expected; moreover, we see that the performance is almost the same for different values of the fading severity (m), and iv) on the contrary, for an unbalanced fading setup, the system behavior is very different. The performance improves when the fading is less severe (a result similar to the uncorrelated system setup), but, very surprisingly, the system performance gets better when the correlation coefficient between the links increases. This latter and apparently unexpected result can be explained as follows. When the wireless links are unbalanced and strongly correlated two favorable conditions for SSK modulation are verified simultaneously: i) the links are more distinguishable from each other due to the unbalanced powers, and ii) the fading fluctuations of each of them change jointly. As a consequence, the fading fluctuations, especially for less severe fading, cannot alter significantly the average power gap (*i.e.*, $\Omega_1 \neq \Omega_2$) between them, thus yielding good system performance. On the other hand, when the links are uncorrelated, but still unbalanced, the links are subject to independent fading fluctuations, which can induce more pronounced variations with respect to the average value, thus yielding worse performance. In other words, deep fades are more likely to offset the average power gap in this case.

In conclusion, the results shown in Figs. 2–5 clearly show that the performance of SSK modulation is significantly affected by the fading scenario. In particular, system scenarios favorable to SSK modulation are characterized by unbalanced fading conditions, which yield better performance and are less sensitive to fading correlation. In the present manuscript, this power unbalance is only due to the wireless channel, since both antennas are assumed to transmit the same average power when they are activated for data transmission. However, unbalanced system setups can be artificially created by allowing each antenna to transmit a different power, according to the fading conditions in each wireless link. In other words, the results shown in this paper suggest that the system performance might be improved by adopting some opportunistic power allocation mechanisms to allow an easier differentiation between the wireless links. Moreover, this could also be a good solution to reduce the effect of channel correlation. In this regard, the analytical frameworks developed in Section III could be the enabling analytical tool for a systematic system optimization of SSK modulation over realistic fading conditions.

V. Conclusion

In this paper, we have proposed an exact analytical framework for analyzing the performance of SSK modulation over correlated Nakagami–*m* fading. Numerical results have validated the accuracy of the proposed analytical derivation and shown that the system performance can change remarkably for various fading conditions. In particular, we have shown that the system performance improves for unbalanced fading scenarios. This result suggests that SSK modulation can be a suitable transmission technology for MIMO systems, and, in particular, for distributed MIMO settings where the transmit–antennas could be geographically far away from each other: a scenario where they are likely to be subject to unbalanced fading fluctuations.

Acknowledgment

We gratefully acknowledge support from the EPSRC (EP/G011788/1) for this work. Harald Haas acknowledges the Scottish Funding Council support of his position within the Edinburgh Research Partnership in Engineering and Mathematics between the University of Edinburgh and Heriot Watt University.

References

[1] Y. Chau and S.–H. Yu, "Space modulation on wireless fading channels", *IEEE Veh. Technol. Conf. – Fall*, vol. 3, pp. 1668–1671, Oct. 2001.

[2] H. Haas, E. Costa, and E. Schultz, "Increasing spectral efficiency by data multiplexing using antennas arrays", *IEEE Int. Symp. Personal, Indoor, Mobile Radio Commun.*, vol. 2, pp. 610–613, Sept. 2002.

[3] Y. Chau and S.–H. Yu, "Space shift keying modulation", *US Patent 9985988*, filed Nov. 7, 2001, granted July 18, 2002.

[4] C.–W. Ahn, S.–B. Yun, E.–S. Kim, H. Haas, R. Y. Mesleh, T.–I. Hyon, and S. McLaughlin, "Spatial modulation method and transmitting and receiving apparatuses using the same in a multiple input multiple output system", *US Patent App. 11822872*, filed July 10, 2007, granted Feb. 14, 2008.

[5] R. Y. Mesleh, H. Haas, S. Sinanovic, C. W. Ahn, and S. Yun, "Spatial modulation", *IEEE Trans. Veh. Technol.*, vol. 57, no. 4, pp. 2228–2241, July 2008.

[6] J. Jeganathan, A. Ghrayeb, and L. Szczecinski, "Spatial modulation: Optimal detection and performance analysis", *IEEE Commun. Lett.*, vol. 12, no. 8, pp. 545–547, Aug. 2008.

[7] J. Jeganathan, A. Ghrayeb, L. Szczecinski, and A. Ceron, "Space shift keying modulation for MIMO channels", *IEEE Trans. Wireless Commun.*, vol. 8, no. 7, pp. 3692–3703, July 2009.

[8] R. Y. Mesleh, I. Stefan, H. Haas, and P. M. Grant, "On the performance of trellis coded spatial modulation", *Int. ITG Workshop on Smart Antennas*, pp. 235–241, Feb. 2009.

[9] A. Alshamali and B. Quza, "Performance of spatial modulation in correlated and uncorrelated Nakagami fading channel", *J. Commun.*, vol. 4, no. 3, pp. 170–174, Ap. 2009.

[10] M. O. Hasna and M.–S. Alouini, "End–to–end performance of transmission systems with relays over Rayleigh–fading channels", *IEEE Trans. Wireless Commun.*, vol. 2, no. 6, pp. 1126–1131, Nov. 2003.

[11] M. Di Renzo, F. Graziosi, and F. Santucci, "A unified framework for performance analysis of CSI-assisted cooperative communications over fading channels", *IEEE Trans. Commun.*, vol. 57, no. 9, pp. 2552–2557, Sept. 2009.

[12] M. Di Renzo, R. Y. Mesleh, H. Haas, and P. M. Grant, "Upper bounds for the analysis of trellis coded spatial modulation over correlated fading channels", *IEEE Veh. Technol. Conf. – Spring*, Taipei, Taiwan, May 2010.

[13] H. L. Van Trees, *Detection, Estimation, and Modulation Theory, Part I: Detection, Estimation, and Linear Modulation Theory*, John Wiley & Sons, Inc. 2001, ISBNs: 0–471–09517–6.

[14] M. Abramowitz and I. A. Stegun, *Handbook of Mathematical Functions with Formulas, Graphs, and Mathematical Tables*, New York, Dover, 9th ed., 1972.

[15] A. P. Prudnikov, Y. A. Brychkov, and O. I. Marichev, *Integrals and Series. Vol. 3: More Special Functions*, 2003.

[16] M. K. Simon and M.–S. Alouini, *Digital Communication over Fading Channels: A Unified Approach to Performance Analysis*, John Wiley & Sons, Inc., 1st ed., 2000.

[17] J. Jeganathan, A. Ghrayeb, and L. Szczecinski, "Generalized space shift keying modulation for MIMO channels", *IEEE Int. Symp. Personal, Indoor, Mobile Radio Commun.*, pp. 1–5, Sept. 2008.

[18] J. Reig, M. A. Martinez–Amoraga, and L. Rubio, "Generation of bivariate Nakagami–*m* fading envelopes with arbitrary not necessary identical fading parameters", *Wireless Commun. and Mobile Computing*, vol. 7, no. 4, pp. 531–537, May 2007.